Open Access Journal

Journal of Power Technologies 94 (2) (2014) 1–11

journal homepage:papers.itc.pw.edu.pl

Analysis of peristaltic flow for a Prandtl fluid model in an endoscope

S. Nadeem*,[a], Hina Sadaf[a], Noreen Sher Akbar[b]

[a]*Department of Mathematics, Quaid-i-Azam University* 45320
Islamabad 44000, *Pakistan*
[b]*DBS&H, CEME, National University of Sciences and Technology*
Islamabad, Pakistan

Abstract

The peristaltic flow of a Prandtl fluid model in an endoscope is analyzed. The flow is modeled in both fixed and wave frame references. We applied the regular perturbation method to solution of the velocity profile. Since it is quite complicated to express pressure rise and frictional forces, numerical integration was used to plot the pressure rise and frictional forces. The effects of various emerging parameters are discussed in respect of pressure rise, friction forces, pressure gradient and streamlines.

Keywords: Peristaltic flow, Endoscope, Regular perturbation method, Prandtl fluid model

1. Introduction

Peristalsis is a system of fluid transfer that is used by numerous systems in the living body to propel or to mix the content of a tube. This mechanism has a broad assortment of applications in industry and physiology, which include urine transfer from kidney to bladder, swallowing food stuff through the esophagus, chyme motion in the gastrointestinal tract, vasomotion of small blood vessels and function of spermatozoa in the human reproductive tract. There are many engineering processes as well in which peristaltic pumps are used to move a wide range of fluids particularly in the chemical and pharmaceutical industries. This mechanism is also used in the transport of slurries, sanitary fluids and noxious fluids in the nuclear industry [1–4]. Brasseur and Lu [5] treated the possessions of a peripherical layer of different viscosity on peristaltic pumping with Newtonian fluid. In another article Li and Brasseur [6] discussed non-steady peristaltic transport in finite-length tubes. They constitute a problem in a steady frame of reference moving with peristaltic waves. The flow of a food-bolus through the esophagus is investigated by Misra and Pandey [7].

An endoscope is an instrument used to observe the interior of a hollow organ or cavity of the body. Hakeem et al. [8, 9] discussed the use of an endoscope for peristaltic flow for a generalized Newtonian fluid with variable viscosity. Peristaltic flow with heat transfer in a vertical porous annulus is presented by Vajravelu et al. [10]. Hayat et al. [11] treated the peristaltic flow for the Newtonian fluid in an endoscope and discussed the exact solution. The Adomian solution for the MHD peristaltic flow of a biofluid with variable viscosity in circular cylindrical tube via application of an endoscope is reported by Ebaid et al. [12]. Nadeem and Akbar [13–17] describe the features of peristaltic flow in an endoscope for different non-Newtonian fluids. Effects of heat transfer and magnetic field for the peristaltic flow of Newtonian fluid in an annulus is analyzed by Mekheimer et

*Corresponding author
Email address: snqau@hotmail.com (S. Nadeem*,)

al. [18]. Recently, Ellahi [19] presented the thermodynamics, stability, applications and techniques of the differential type. A few other significant studies relating to the features of peristalsis are cited in [20–23].

The theme of the present article is to discuss the analysis of peristaltic flow for a Prandtl fluid model in an endoscope. The flow equations for the anticipated fluid model are developed in both a fixed and moving frame of references. Analytical solutions were constructed using the perturbation method for the velocity profile. Since it is quite complicated to express pressure rise and frictional forces, numerical integration was used to plot the pressure rise and frictional forces. The effects of various emerging parameters are discussed in respect of pressure rise, friction forces, pressure gradient and streamlines.

2. Mathematical model

For an incompressible fluid the balance of mass and momentum are given by

$$div\bar{\mathbf{V}} = 0, \tag{1}$$

$$\rho\frac{d\bar{\mathbf{V}}}{d\bar{t}} = div\bar{\mathbf{T}}+\rho\mathbf{f}, \tag{2}$$

where ρ is the density, $\bar{\mathbf{V}}$ is the velocity vector, $\bar{\mathbf{T}}$ is the Cauchy stress tensor.

$$\bar{\mathbf{T}} = -\bar{P}\mathbf{I} + \bar{\mathbf{S}} \tag{3}$$

where $\bar{\mathbf{S}}$ is the extra stress tensor of Prandtl fluid model [17]. The nonzero stress component is defined in the proceeding section.

3. Mathematical formulation

Let us consider the peristaltic transport of a two dimensional and incompressible Prandtl fluid in an endoscope. The inner tube is rigid and the outer tube has a sinusoidal wave traveling down its walls. The geometry of the wall surface (Fig. 1) is defined as

$$\bar{R}_1 = a_1, \tag{4}$$

$$\bar{R}_2 = a_2 + b\sin\frac{2\pi}{\lambda}\left(\bar{Z} - c\bar{t}\right), \tag{5}$$

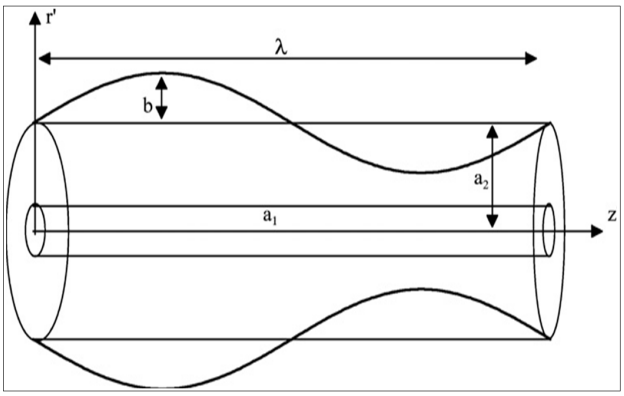

Figure 1: Flow geometry

where a_1 is the radius of the inner tube, a_2 is the radius of the outer tube at inlet, b is the wave amplitude, λ wave length, c is the wave speed and $\bar{t}$ the time. The governing equations in the fixed frame for a two dimensional and incompressible Prandtl fluid model are given as

$$\frac{\partial\bar{U}}{\partial\bar{R}} + \frac{\bar{U}}{\bar{R}} + \frac{\partial\bar{W}}{\partial\bar{Z}} = 0, \tag{6}$$

$$\begin{gathered}\rho\left[\frac{\partial\bar{U}}{\partial\bar{t}} + \bar{U}\frac{\partial\bar{U}}{\partial\bar{R}} + \bar{W}\frac{\partial\bar{U}}{\partial\bar{Z}}\right] = \\ -\frac{\partial\bar{P}}{\partial\bar{R}} + \frac{1}{\bar{R}}\frac{\partial\left(\bar{R}\bar{S}_{\bar{R}\bar{R}}\right)}{\partial\bar{R}} + \frac{\partial\left(\bar{S}_{\bar{R}\bar{Z}}\right)}{\partial\bar{Z}} - \frac{\bar{S}_{\bar{\theta}\bar{\theta}}}{\bar{R}},\end{gathered} \tag{7}$$

$$\rho\left(\frac{\partial\bar{W}}{\partial\bar{t}} + \bar{U}\frac{\partial\bar{W}}{\partial\bar{R}} + \bar{W}\frac{\partial\bar{W}}{\partial\bar{Z}}\right) = -\frac{\partial\bar{P}}{\partial\bar{Z}} + \frac{1}{\bar{R}}\frac{\partial\left(\bar{R}\bar{S}_{\bar{R}Z}\right)}{\partial\bar{R}} + \frac{\partial\left(\bar{S}_{\bar{Z}\bar{Z}}\right)}{\partial\bar{Z}}. \tag{8}$$

In the above equations, $\bar{P}$ is the pressure and $\bar{U}$, $\bar{W}$ are the respective velocity components in the radial and axial directions respectively. In the fixed coordinates ($\bar{R}$, $\bar{Z}$), the flow between the two tubes is unsteady. It becomes steady in a wave frame ($\bar{r}$, $\bar{z}$) moving with same speed as the wave moves in the $\bar{Z}$ directions. The transformations between the two frames are

$$\bar{r} = \bar{R}, \quad \bar{z} = \bar{Z} - c\bar{t}, \quad \bar{u} = \bar{U}, \quad \bar{w} = \bar{W} - c. \tag{9}$$

The appropriate boundary conditions in the wave frame are defined as

$$\begin{gathered}\bar{w} = -c, \quad at\ \bar{r} = \bar{r}_1, \quad \bar{w} = -c\ at, \\ \bar{r} = \bar{r}_2 = a_2 + b\sin\tfrac{2\pi}{\lambda}(\bar{z}).\end{gathered} \tag{10}$$

Introducing the dimensionless variables

$$\begin{gathered} R=\frac{\bar{R}}{a_2},\ r=\frac{\bar{r}}{a_2},\ Z=\frac{\bar{Z}}{\lambda},\ z=\frac{\bar{z}}{\lambda},\ W=\frac{\bar{W}}{c}, \\ w=\frac{\bar{w}}{c},\ U=\frac{\lambda\bar{U}}{a_2 c},\ u=\frac{\lambda\bar{u}}{a_2 c},\ p=\frac{a_2^2\bar{p}}{c\lambda\eta},\ \delta=\frac{a_2}{\lambda}, \\ \phi=\frac{b}{a}<1,\ t=\frac{c\bar{t}}{\lambda},\ Re=\frac{\rho c a_2}{\eta},\ S_{rr}=\frac{a_2\bar{S}_{rr}}{c\eta},\ S_{rz}=\frac{a_2\bar{S}_{rz}}{c\eta}, \\ S_{zz}=\frac{a_2\bar{S}_{zz}}{c\eta},\ S_{\theta\theta}=\frac{a_2\bar{S}_{\theta\theta}}{c\eta},\ r_1=\frac{\bar{r}_1}{a_2}=\frac{a_1}{a_2}=\varepsilon,\ \alpha=\frac{A}{\eta c^*}, \\ \beta=\frac{Ac^2}{6a_2^2\eta c^{*3}},\ r_2=\frac{\bar{r}_2}{a_2}=1+\phi\sin(2\pi z). \end{gathered} \tag{11}$$

Using Eqs. (9) and (11) in Eqs. (6) to (8), we obtain

$$\frac{\partial u}{\partial r}+\frac{u}{r}+\frac{\partial w}{\partial z}=0, \tag{12}$$

$$\begin{gathered} \delta^3 R_e\left(u\frac{\partial u}{\partial r}+w\frac{\partial u}{\partial z}\right)= \\ -\frac{\partial p}{\partial r}+\delta^2\frac{\partial}{\partial z}(S_{rz})+\frac{\delta}{r}\frac{\partial}{\partial r}(rS_{rr})-\frac{\delta}{r}S_{\theta\theta}, \end{gathered} \tag{13}$$

$$\delta R_e\left(u\frac{\partial w}{\partial r}+w\frac{\partial w}{\partial z}\right)=-\frac{\partial p}{\partial z}+\frac{1}{r}\frac{\partial}{\partial r}(rS_{rz})+\delta\frac{\partial}{\partial z}(S_{zz}). \tag{14}$$

Under the assumptions of long wave length $\delta < 1$ and low Reynolds number, neglecting the terms of order δ and higher, Eqs. (13) and (14) take the form

$$\frac{\partial p}{\partial r}=0, \tag{15}$$

$$\frac{\partial p}{\partial z}=\frac{1}{r}\frac{\partial}{\partial r}\left[r(S_{rz})\right], \tag{16}$$

where S_{rz} component given below are obtained by making use of Eq. (9) and (11) in the stress tensor given in [17]

$$S_{rz}=\alpha\left(\frac{\partial w}{\partial r}\right)+\beta\left(\frac{\partial w}{\partial r}\right)^3 \tag{17}$$

Eq. (15) shows that p is not a function of r. The corresponding dimensionless boundary conditions for the problem under consideration are defined as

$$\begin{gathered} w=-1\ at\ r=r_1=\varepsilon, \\ w=-1\ at\ r=r_2=1+\phi\sin(2\pi z). \end{gathered} \tag{18}$$

4. Solution of the problem

To find the solution of Eq. (16), we employ the regular perturbation method. For the regular perturbation solution, we expand w, F and p as

$$\begin{aligned} w&=w_0+\beta w_1+..., \\ F&=F_0+\beta F_1+..., \\ p&=p_0+\beta p_1+..., \end{aligned} \tag{19}$$

The resulting expression for the velocity field is defined as

$$\begin{gathered} w=-1+\frac{dp}{dz}\frac{1}{4\alpha}\left(r^2+a_1\ln r+a_2\right) \\ +\beta\left(a_4 r^4+a_5 r^2+a_9+\frac{1}{r^2}a_7+a_{10}\ln r\right). \end{gathered} \tag{20}$$

The dimensionless time mean flow rate F_i, pressure rise Δp and friction force (at the wall) on the inner and outer tubes are F^0 and F^1 in non-dimensional forms are defined as

$$F_0=\int_{r_1}^{r_2} rw_0 dr,\quad F_1=\int_{r_1}^{r_2} rw_1 dr, \tag{21}$$

$$\begin{gathered} \Delta p=\int_0^1\left(\frac{dp}{dz}\right)dz,\ F^0=\int_0^1 r_1^2\left(-\frac{dp}{dz}\right)dz, \\ F^1=\int_0^1 r_2^2\left(-\frac{dp}{dz}\right)dz. \end{gathered} \tag{22}$$

From Eq. (21), we have

$$\frac{dp_0}{dz}=\frac{4\alpha(F_0-a_{11})}{a_{12}},\quad \frac{dp_1}{dz}=\frac{4\alpha(F_1-a_{13})}{a_{12}}, \tag{23}$$

whereas pressure gradient in the combined form can be obtained by using the relation of Eq. (23) and Eq. (19)

$$\frac{dp}{dz}=Fa_{15}+a_{14}. \tag{24}$$

Flow rate in dimensionless form can be defined as

$$Q=F+\frac{1}{2}\left(1+\frac{\phi^2}{2}-\varepsilon^2\right), \tag{25}$$

Velocities in terms of stream functions are defined as

$$u=\frac{-1}{r}\left(\frac{\partial\Psi}{\partial z}\right)\ and\ w=\frac{1}{r}\left(\frac{\partial\Psi}{\partial r}\right). \tag{26}$$

Making use of Eq. (20) in Eq. (26), we obtain a stream function as

$$\Psi = \frac{-r^2}{2} + \frac{dp}{dz}\frac{1}{4\alpha}\left(\frac{r^4}{4} + a_1\left(\frac{r^2\ln r}{2} - \frac{r^2}{4}\right) + a_2\frac{r^2}{2}\right) + \beta\left(\frac{a_4 r^6}{6} + \frac{a_5 r^4}{4} + a_{10}\left(\frac{r^2\ln r}{2} - \frac{r^2}{4}\right) + \frac{a_9 r^2}{2} + a_7\ln r\right). \quad (27)$$

For analysis, we considered five wave forms namely, sinusoidal wave, triangular wave, square wave, trapezoidal wave, multisinusoidal wave. The non-dimensional expressions for these wave forms are given as

1. Sinusoidal wave:

$$r_2(z) = 1 + \phi\sin(2\pi z), \quad (28)$$

2. Triangular wave:

$$r_2(z) = 1 + \phi\left\{\frac{8}{\pi^3}\sum_{n=1}^{\infty}\frac{(-1)^{n+1}}{(2n-1)}\sin(2\pi(2n-1)z)\right\}, \quad (29)$$

3. Square wave:

$$r_2(z) = 1 + \phi\left\{\frac{4}{\pi}\sum_{n=1}^{\infty}\frac{(-1)^{n+1}}{(2n-1)}\cos(2\pi(2n-1)z)\right\}, \quad (30)$$

4. Trapezoidal wave:

$$r_2(z) = 1+ \phi\left\{\frac{32}{\pi^2}\sum_{n=1}^{\infty}\frac{\sin\frac{\pi}{8}(2n-1)}{(2n-1)^2}\sin(2\pi(2n-1)z)\right\}, \quad (31)$$

5. Multisinusoidal wave:

$$r_2(z) = 1 + \phi\sin(2m\pi z). \quad (32)$$

The expression for pressure rise Δp and the friction forces are calculated numerically by using mathematics software, whereas the constants appeared in the last section.

5. Graphical results and discussion

In this section the graphical result of the Prandtl fluid model is presented. The expressions for pressure rise and friction forces are calculated numerically. Figs. 2a, 3a and 4a show the pressure rise (versus flow rate) for different values of ϕ (amplitude ratio) α and β (fluid parameters). From these figures it is observed that in the range ($Q\varepsilon$[-2,-0.01]) by increasing the values of ϕ, α and β pressure rise increases and in the range ($Q\varepsilon$[0.01, 2]) pressure decreases with the increase of ϕ, α and β. Moreover retrograde pumping regions are $Q\varepsilon$[-2,-0.01]. The free pumping region can also be seen in Figs. 1, 4 and 7 when $Q = 0$, and $\Delta P = 0$ otherwise it is augmented pumping. Figs. 2b, 2c, 3b, 3c, 4b, 4c shows the friction forces (inner and outer tube) for different values of ϕ, α and β. From these figures it is observed that the inner and outer friction force exhibits an opposite behavior comparative to pressure rise. For the fixed values of the parameters, inner friction force behaves in a similar way as the outer friction force. Also for the fixed values of the parameters, the outer friction force is larger than the inner friction force. We drew five waveforms for the analysis of pressure gradient and streamlines. A waveform that undergoes a change of shape, returns to its original shape, and repeats with the same pattern of changes is known as a periodic waveform. Periodic waveforms are nonsinusoidal except for the sine wave and the periodic waveforms that will be discussed here are the sine wave, square wave, multisinusoidal wave, trapezoidal wave and triangular wave. These waves are important because they retain their wave shape. These waves play a vital role in many mathematical equations, including self-oscillatory systems, excitable systems and reaction-diffusion-advection systems and take many shapes in the human body. Equations of these types are widely used as mathematical models of chemistry, biology and physics. Fig. 5 presents the pressure gradient for various values of ϕ. For different wave forms it is observed from figure 5, (a, c, d) having region ($z\varepsilon$[0.5, 0.99] and $z\varepsilon$[1.51, 2]) the pressure gradient is lesser and a huge pressure gradient occurs in the region $z\varepsilon$[1, 1.50]. Fig. 5b, shows that in the region ($z\varepsilon$[0.77, 0.99] and $z\varepsilon$[1.27, 1.50]) pressure gradient is small and the large pressure gradient occur in the region ($z\varepsilon$[0.5, 0.76] and $z\varepsilon$[1, 1.26] $z\varepsilon$[1.51, 1.76]). Fig. 5e, shows that in the region $z\varepsilon$[0.75, 1.25], the pressure gradient is large and a small pressure gradient occurs in the region $z\varepsilon$[1.26, 1.75]. One explanation of from these figures is that in the wider portion of the endoscopic tube the pressure gradient is comparatively small so the flow can easily pass

without a large pressure gradient, whereas in the narrow portion of the tube a much larger pressure gradient is required to maintain the same flux. This is in good agreement with the physical conditions. Trapping is an interesting phenomenon, where a bolus is transported at the wave speed and this trapped bolus is pushed ahead along the peristaltic wave. Fig. 6 show the streamlines for the sinusoidal wave, square wave, trapezoidal wave, triangular wave and multisinusoidal wave. It is depicted from these figures that the size of the trapping bolus in triangular wave is small related to the other waves.

6. Conclusion

The main points are summarized as follows:

1. There is an opposite behavior between pressure rise and the frictional forces.
2. Inner and outer frictional forces show the same behavior.
3. The pressure gradient increases with an increase in ϕ for all five wave shapes.
4. The size of the trapping bolus in triangular wave is smaller than in the compared to the other waves.

References

[1] O. Eytan, D. Elad, Analysis of intra-uterine fluid motion induced by uterine contractions, Bull Math Biol. 61 (2) (1999) 221–238.

[2] M. Y. Jaffrin, A. H. Shaprio, Peristaltic pumping, Ann. Rev. Fluid Mech 3 (1971) 13–36.

[3] V. Seshadri, Z. Hasan, B. B. Gupta, Peristaltic pumping in non-uniform distensible tubes with different wave forms, J. Biophys Et Med Nucl 8 (1984) 9–14.

[4] C. Pozrikidis, A study of peristaltic flow, J. of Fluid Mechanics 180 (1987) 515–527.

[5] S. Brasseur, N. Q. Lu, The influence of a peripherical layer of different viscosity on peristaltic pumping with newtonian fluid, J. of Fluid Mechanics 174 (1987) 495–519.

[6] M. Li, J. G. Brasseur, Non-steady peristaltic transport in finite-length tubes, J. of Fluid Mechanics 248 (1993) 129–151.

[7] J. C. Misra, S. K. Pandey, A mathematical model for oesophageal swallowing of a food-bolus, Mathematical and Computer Modelling 33 (8–9) (2001) 997–1009.

[8] A. El. Hakeem, A. El-Naby, A. E. M. El-Misiery, Effects of an endoscope and generalized newtonian fluid on peristaltic motion, Applied Mathematics and Computation 128 (1) (2002) 19–35.

[9] A. El. Hakeem, A. EI. Naby, A. E. M. El. Misery, I. I. El Shamy, Effects of an endoscope and fluid with variable viscosity on peristaltic motion, Applied Mathematics and Computation 158 (2) (2004) 497–511.

[10] K. Vajravelu, G. Radhakrishnamacharya, V. Radhakrishnamurty, Peristaltic flow and heat transfer in a vertical porous annulus with long wave approximation, International Journal of Non-Linear Mechanics 42 (5) (2007) 754–759.

[11] T. Hayat, N. Ali, S. Asghar, A. M. Siddiqui, Exact peristaltic flow in tubes with an endoscope, Applied Mathematics and Computation 182 (1) (2006) 359–368.

[12] A. Ebaid, A new numerical solution for the mhd peristaltic flow of a biofluid with variable viscosity in circular cylindrical tube via adomian decomposition method, Physics Letters A 372 (32) (2008) 5321–5328.

[13] S. Nadeem, N. S. Akbar, Influence of temperature dependent viscosity on peristaltic transport of a newtonian fluid: Application of an endoscope, Applied Mathematics and Computation 216 (2010) 3606–3619.

[14] S. Nadeem, N. S. Akbar, S. Ashiq, Simulation of heat and chemical reactions on the peristaltic flow of a johnson segalman fluid in an endoscope, International Journal of Nonlinear Sciences and Numerical Simulation 11 (10) (2010) 871–883.

[15] S. Nadeem, N. S. Akbar, K. Vajravelue, Peristaltic flow of a sisko fluid in an endoscope analytical and numerical solutions, Int. J. of Comput. Math 88 (2011) 1013–1023.

[16] N. S. Akbar, S. Nadeem, Characteristics of heating scheme and mass transfer on the peristaltic flow for an eyring-powell fluid in an endoscope, International Journal of Heat and Mass Transfer 55 (1–3) (2012) 375–383.

[17] N. S. Akbar, S. Nadeem, C. Lee, Peristaltic flow of a prandtl fluid model in an asymmetric channel, International Journal of Physical Sciences 7 (5) (2012) 687–695.

[18] K. Mekheimer, Y. A. elmaboud, The influence of heat transfer and magnetic field on peristaltic transport of a newtonian fluid in a vertical annulus application of an endoscope, Physics Letters A 372 (10) (2008) 1657–1665.

[19] R. Ellahi, The thermodynamics, stability, applications and techniques of differential type a review, Reviews in Theoretical Science 2 (8) (2014) 116–123.

[20] A. A. Khan, R. Ellahi, M. Usman, The effects of variable viscosity on the peristaltic flow of non-newtonian fluid through a porous medium in an inclined channel with slip boundary conditions, Journal of Porous Media 16 (1) (2013) 59–67.

[21] A. A. Khan, R. Ellahi, K. Vafai, Peristaltic transport of jeffrey fluid with variable viscosity through a porous medium in an asymmetric channel, Advances in Mathematical Physics 2012 (2012) 1–15.

[22] S. Hina, T. Hayat, S. Asghar, A. A. Hendi, Influence of compliant walls on peristaltic motion with heat/mass transfer and chemical reaction, International Journal of Heat and Mass Transfer 55 (13–14) (2012) 3386–3394.

[23] D. Tripathi, Study of transient peristaltic heat flow

through a finite porous channel, Mathematical and Computer Modelling 57 (5–6) (2013) 1270–1283.

Appendix

$$a_1 = \frac{-\left(r_1^2 - r_2^2\right)}{\ln r_1 - \ln r_2},\ a_2 = -\frac{\left(r_1^2 \ln r_2 - r_2^2 \ln r_1\right)}{\ln r_2 - \ln r_1},\ a_3 = -\frac{1}{\alpha}\left(\frac{1}{4\alpha}\frac{dp_0}{dz}\right)^3,$$

$$a_4 = 2a_3,\ a_5 = 6a_1a_3,\ a_6 = 6a_1^2a_3,\ a_7 = \frac{-a_3a_1^3}{2},$$

$$a_8 = \frac{-\alpha\left(a_4\left(r_1^4 - r_2^4\right) + a_5\left(r_1^2 - r_2^2\right) + a_7\left(\frac{1}{r_1^2} - \frac{1}{r_2^2}\right) + a_6\left(\ln r_1 - \ln r_2\right)\right)}{\ln r_1 - \ln r_2},$$

$$a_9 = \frac{a_4\left(r_1^4 \ln r_2 - r_2^4 \ln r_1\right)}{\ln r_{1-} \ln r_2} + a_2a_5 - \frac{a_7\left(\frac{\ln r_2}{r_1^2} - \frac{\ln r_1}{r_2^2}\right)}{\ln r_{2-} \ln r_1},$$

$$a_{10} = a_6 + \frac{a_8}{\alpha},\ a_{11} = -\frac{\left(r_2^2 - r_1^2\right)}{2},$$

$$a_{12} = \frac{1}{4}\left(r_2^4 - r_1^4\right) + a_1\left(\frac{r_2^2 \ln r_2 - r_1^2 \ln r_1}{2} - \frac{\left(r_2^2 - r_1^2\right)}{4}\right) + \frac{a_2\left(r_2^2 - r_1^2\right)}{2},$$

$$a_{13} = \frac{a_4}{6}\left(r_2^6 - r_1^6\right) + \frac{a_5}{4}\left(r_2^4 - r_1^4\right) + a_{10}\left(\frac{r_2^2 \ln r_{2-} r_1^2 \ln r_1}{2} - \frac{\left(r_2^2 - r_1^2\right)}{4}\right) + \frac{a_9}{2}\left(r_2^2 - r_1^2\right) + a_7\left(\ln r_2 - \ln r_1\right).$$

$$a_{14} = \frac{-4\alpha a_{11}}{a_{12}} - \frac{4\beta\alpha a_{13}}{a_{12}},\ a_{15} = \frac{4\alpha}{a_{12}}.$$

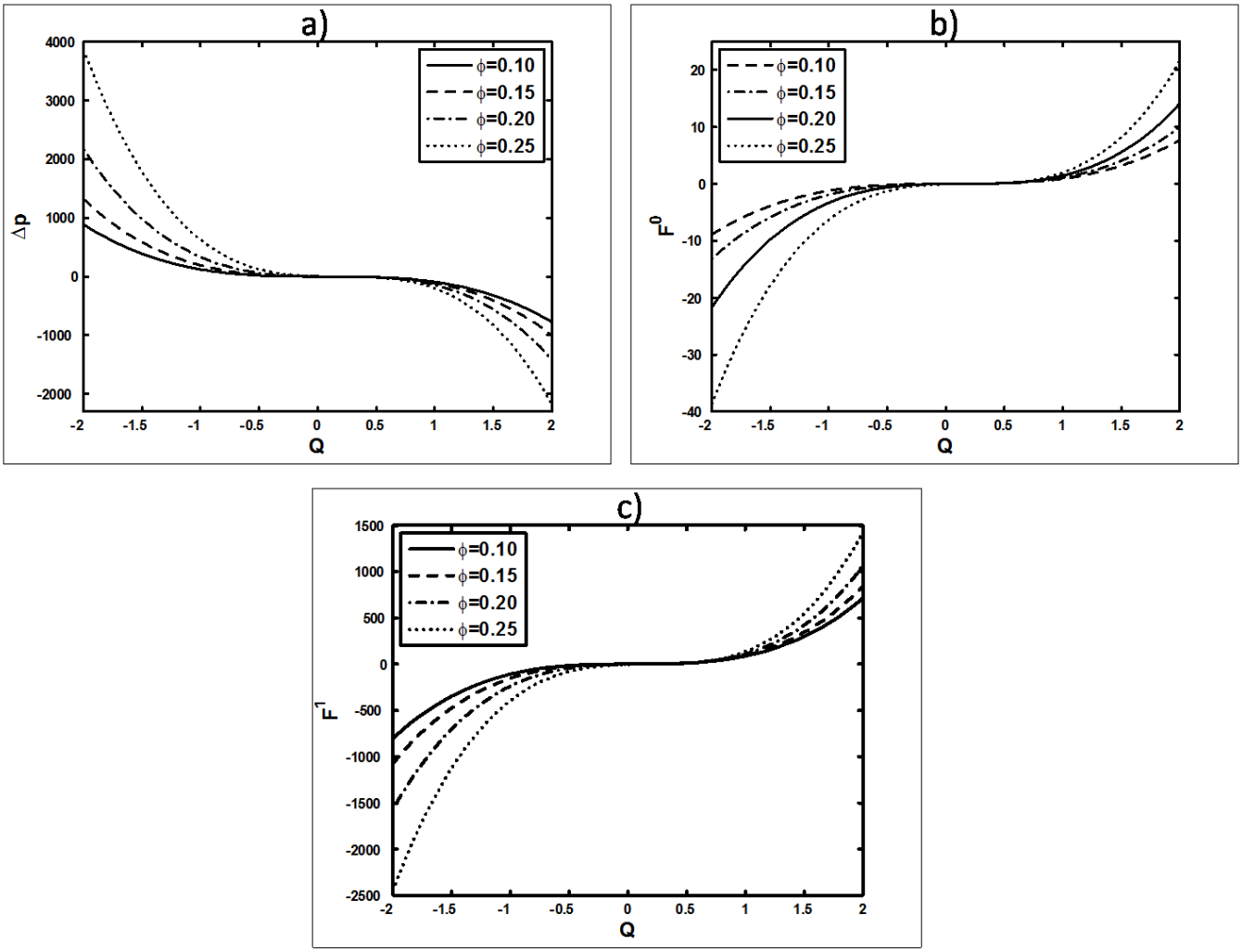

Figure 2: (a) Pressure rise; (b) Frictional forces for inner tube; (c) Frictional forces for outer tube for $\varepsilon = 0.1$, $\alpha = 0.05$, $\beta = 0.02$.

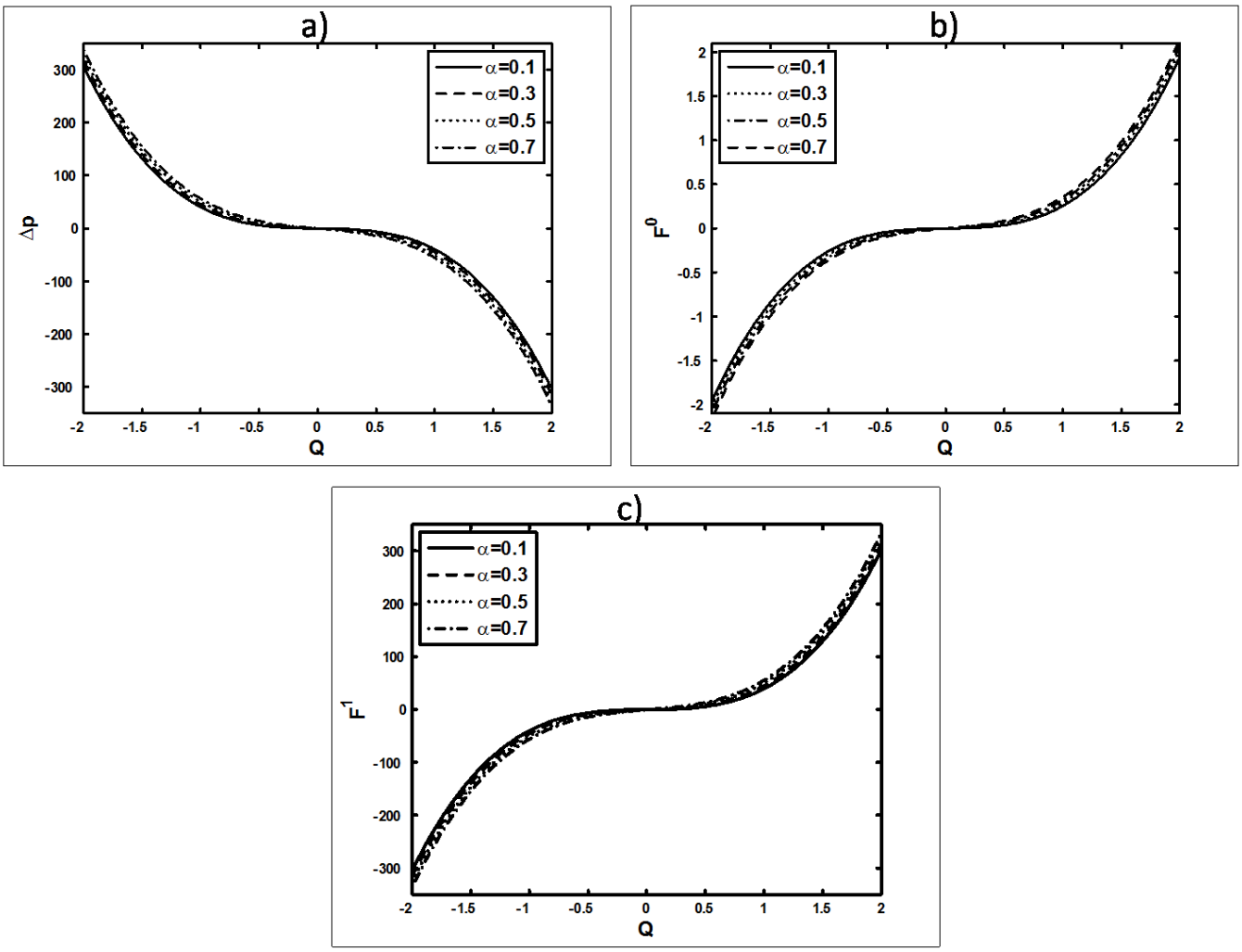

Figure 3: (a) Pressure rise; (b) Frictional forces for inner tube; (c) Frictional forces for outer tube for $\varepsilon = 0.08$, $\phi = 0.02$, $\beta = 0.01$.

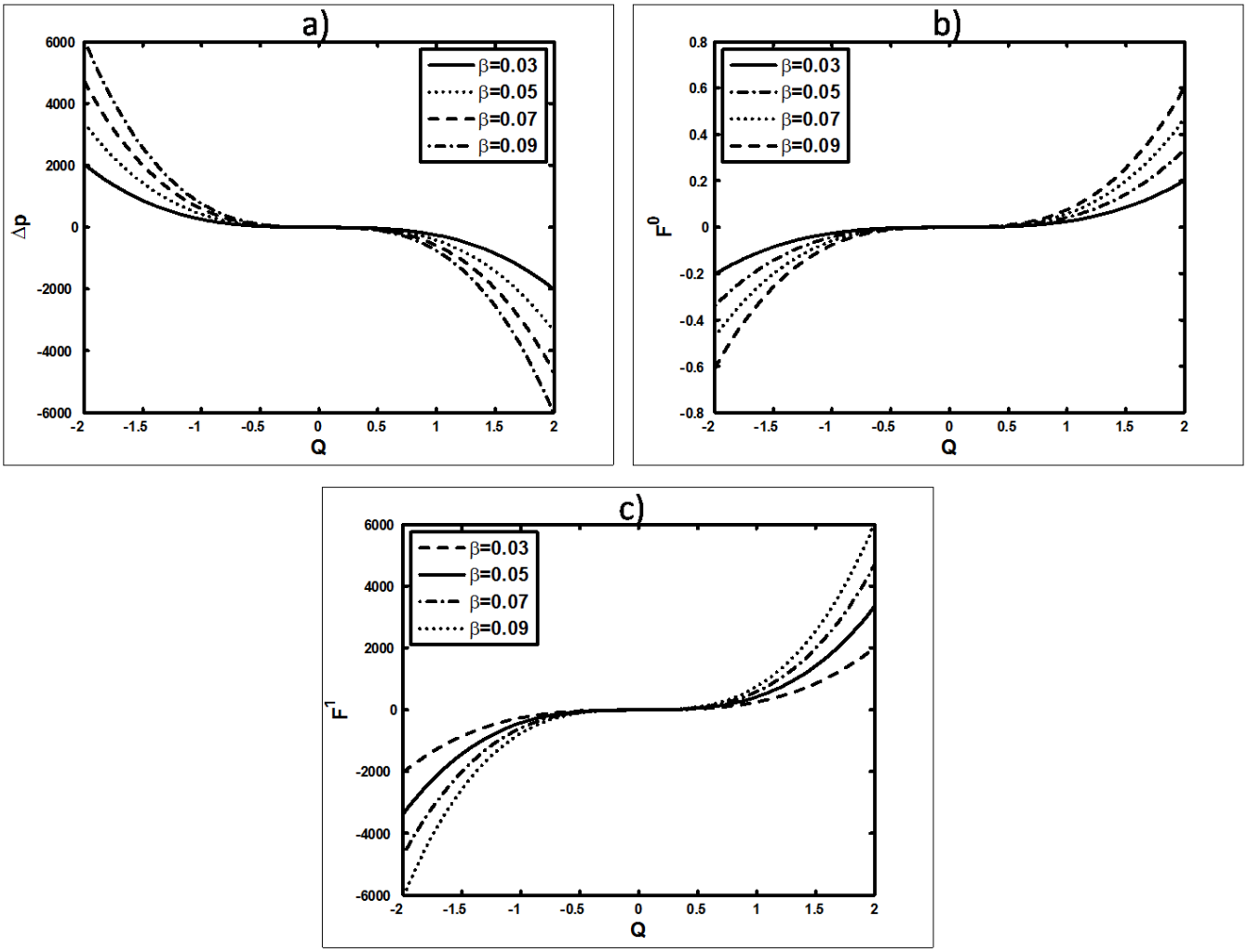

Figure 4: (a) Pressure rise; (b) Frictional forces for inner tube; (c) Frictional forces for outer tube for $\varepsilon = 0.01$, $\phi = 0.02$, $\alpha = 0.15$.

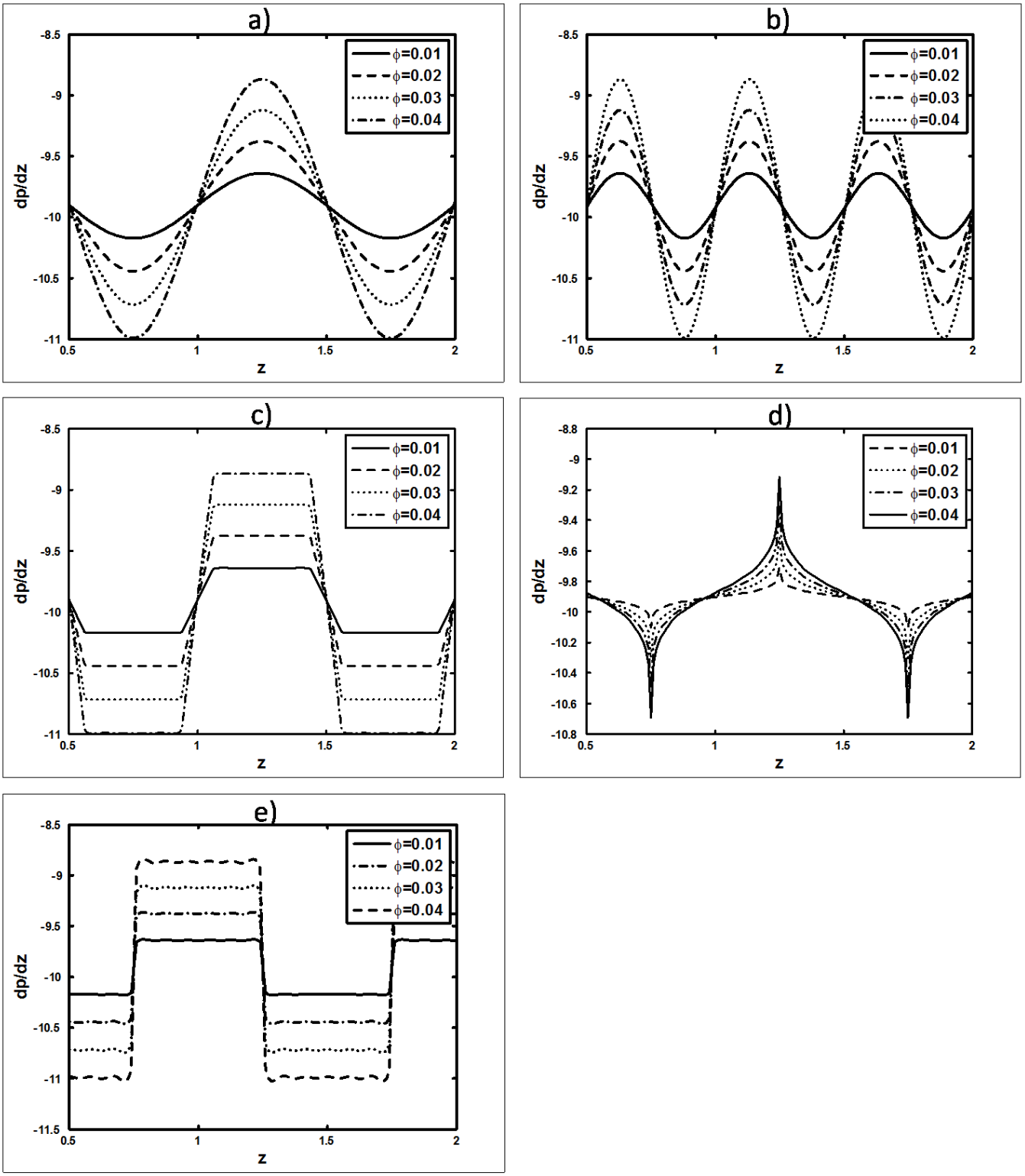

Figure 5: (a, b) Pressure gradient for (Sinusoidal wave) (Multisinusoidal wave) $\varepsilon = 0.09$, $Q = 0.4$, $\beta = 0.04$, $\alpha = 0.02$, $m = 1.99$; (c, d) Pressure gradient for (Trapezoidal wave) (Triangular wave) $\varepsilon = 0.09$, $Q = 0.4$, $\beta = 0.04$, $\alpha = 0.02$; (e) Pressure gradient for $\varepsilon = 0.09$, $Q = 0.4$, $\beta = 0.04$, $\alpha = 0.02$.

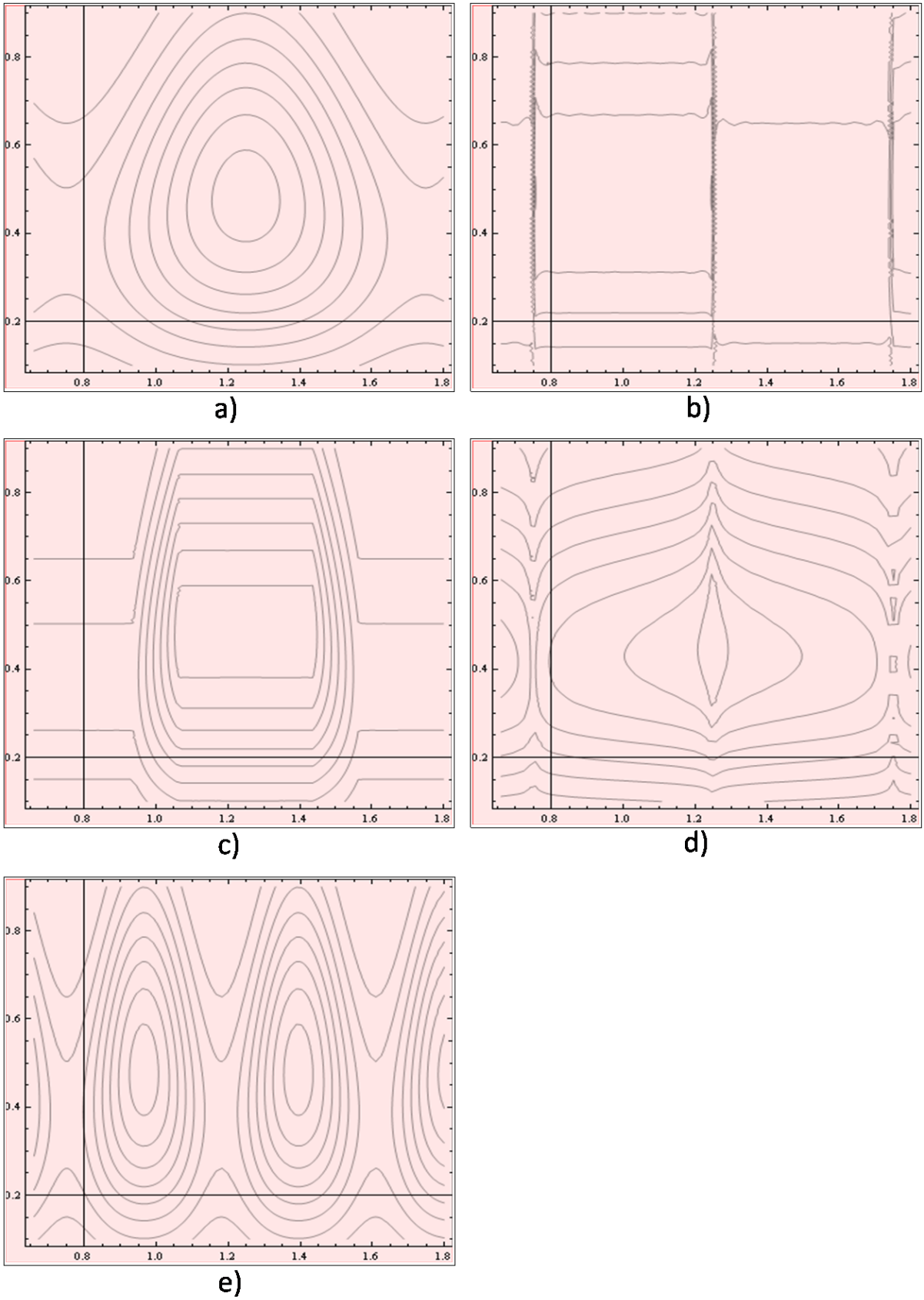

Figure 6: (a, b) shows the Streamlines for (Sinusoidal wave) (Square wave) for $\varepsilon = 0.03$, $Q = 0.31$, $\beta = 0.32$, $\alpha = 0.02$, $\phi = 0.12$; (c, d) shows the Streamlines for (Trapezoidal wave) (Triangular wave) for $\varepsilon = 0.03$, $Q = 0.31$, $\beta = 0.32$, $\alpha = 0.02$, $\phi = 0.12$; (e) shows the Streamlines for (Multisinusoidal wave) for $\varepsilon = 0.03$, $Q = 0.31$, $\beta = 0.32$, $\alpha = 0.02$, $\phi = 0.12$, $m = 2.33$.